Four distinct pathways of hemoglobin uptake in the malaria parasite *Plasmodium falciparum*

David A. Elliott*[†], Michael T. McIntosh[‡], H. Dean Hosgood III[§], Shuo Chen*, Gina Zhang*, Pavlina Baevova[¶], and Keith A. Joiner*

*Department of Cell Biology and Anatomy, University of Arizona College of Medicine, Tucson, AZ 85724; and Departments of [‡]Internal Medicine, [§]Epidemiology and Public Health, and [¶]Laboratory Medicine, Yale University School of Medicine, New Haven, CT 06520

During the bloodstage of malaria infection, the parasite internalizes and degrades massive amounts of hemoglobin from the host red blood cell. Using serial thin-section electron microscopy and three-dimensional reconstruction, we demonstrate four independent, but partially overlapping, hemoglobin-uptake processes distinguishable temporally, morphologically, and pharmacologically. Early ring-stage parasites undergo a profound morphological transformation in which they fold, like a cup, onto themselves and in so doing take a large first gulp of host cell cytoplasm. This event, which we term the "Big Gulp," appears to be independent of actin polymerization and marks the first step in biogenesis of the parasite's lysosomal compartment—the food vacuole. A second, previously identified uptake process, uses the cytostome, a well characterized and morphologically distinct structure at the surface of the parasite. This process is more akin to classical endocytosis, giving rise to small (<0.004 fl) vesicles that are marked by the early endosomal regulatory protein Rab5a. A third process, also arising from cytostomes, creates long thin tubes previously termed cytostomal tubes in an actin-dependent manner. The fourth pathway, which we term phagotrophy, is similar to the Big Gulp in that it more closely resembles phagocytosis, except that phagotrophy does not require actin polymerization. Each of these four processes has aspects that are unique to *Plasmodium*, thus opening avenues to antimalarial therapy.

actin | endocytosis | food vacuole | cytosome | transport

Malaria afflicts 300–500 million people each year and causes >1 million deaths (World Health Organization). The majority of fatalities represent children under age 5 infected by *Plasmodium falciparum*, an obligate intracellular parasite that causes the most severe malaria.

Morbidity and mortality result from the asexual replication of *Plasmodium* in the blood stream of the human host. As the parasite progresses within the host red blood cell from the immature ring stage to the trophozoite stage and then to the replicating schizont stage, massive amounts of hemoglobin from the red blood cell cytosol are internalized (1). The internalized hemoglobin is ultimately digested in a compartment termed the food vacuole (FV) (2). The toxic heme moiety released from the digested hemoglobin is detoxified by its polymerization and sequestration as an inert crystalline deposit known as hemozoin (3). Both hemoglobin metabolism and heme detoxification are essential features of parasite biology (4). Blocking either process is lethal to the organism and is the basis for both currently available and experimental therapies.

Compared with our understanding of the hemoglobin degradation process, our understanding of the hemoglobin-uptake and -transport processes is minimal (5, 6). It is generally agreed that uptake of hemoglobin from the red cell occurs via the cytostome and that this internalized hemoglobin is primarily digested in the FV. However, no consensus exists regarding the morphology, the temporal sequence of events, or the membrane transport machinery required for hemoglobin uptake and transport. Much of this uncertainty derives from the unique nature of the host cell and the parasite itself. Red blood cells lack internal structure, and the

parasite itself has little defined internal organization. Thus, in any particular two-dimensional image of the parasite or the host cell, it is nearly impossible to determine the position or orientation of anatomical features (7, 8). It is likewise difficult to relate different images to one another to map the morphologic and temporal sequence of hemoglobin uptake and delivery to the FV. For example, although tubular hemoglobin-containing structures, when viewed in cross section, cannot be distinguished from spherical vesicles, the literature is dominated by the assumption that discrete spherical vesicles mediate hemoglobin transport.

Using analyses performed in three dimensions of >200 complete parasites, and with a serial fine ultrastructural method developed for this study [ref. 9 and supporting information (SI) *Materials and Methods*], we here elucidate the morphological and temporal sequence of events involved in delivering hemoglobin from the red blood cell cytosol to the FV. We differentiate four distinct hemoglobin-uptake structures and characterize regulatory molecules involved in hemoglobin uptake. Because all of these structures have unique mechanistic features, this work suggests several therapeutic targets.

Results

The volume and shape of all completely enclosed hemoglobin-containing structures within the parasite were measured at different points along the intraerythrocytic parasite-development pathway. All measurements were obtained by using a serial fine ultrastructural method that we developed for three-dimensional analyses. As described in *Materials and Methods*, parasites were embedded for transmission electron microscopy (TEM), serially sectioned (SI Movie 1) (9) and segmented (SI Fig. 5 and SI Movie 2), and the volumes of structures were determined. Within each parasite, various organellar compartments were measured for volume and characterized, by using previous conventions (10, 11), as hemoglobin-containing vacuoles (HVs) confirmed by immuno-TEM (SI Fig. 6) or as FVs (hemozoin-containing).

Ring-Stage Parasites Take Up a Single Large Vacuole of Hemoglobin—the Big Gulp. During the first 18–30 h after invasion of a red blood cell, the parasite is in the ring stage, defined morphologically as not having hemozoin visible with a light microscope. Ring-stage parasites can be divided into two populations: those that do not contain a large HV and those that do. Shortly after a merozoite-stage parasite invades the red blood cell, it flattens out and forms a biconcave disk (Fig. 1 *A* and *B*). The parasite, including the
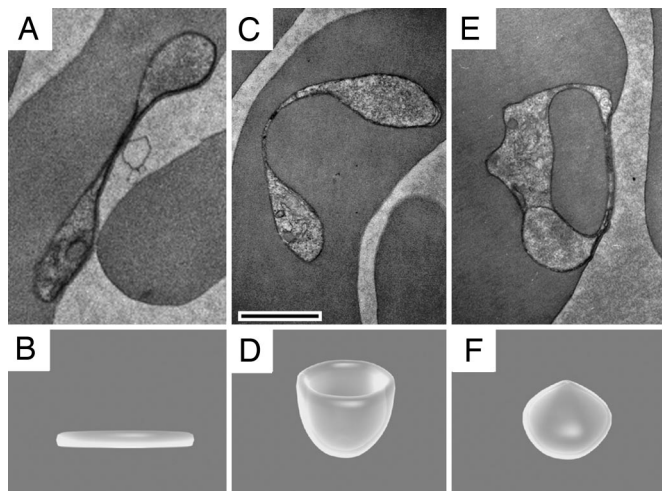

CELL BIOLOGY

Fig. 1. Hemoglobin uptake by the Big Gulp. (*A*, *C*, and *E*) TEM images showing the Big Gulp, in which the parasite forms a single large vacuole filled with hemoglobin. (*B*, *D*, and *F*) Illustrations showing the shape of the ring-stage parasite throughout the Big Gulp process. (*A* and *B*) The ring-stage parasite as it appears shortly after red blood cell invasion when it has flattened and taken on a biconcave disk shape. The parasite then takes on the shape of a cup (*C* and *D*). (*E* and *F*) Completion of the Big Gulp when the parasite has taken a single large vacuole filled with hemoglobin. (Scale bar, 0.5 μm.) Fig. 2 shows that this vacuole can be as large as 40% of the parasite volume. SI Movies 3–6 show four full serial sectioned rings at different stages of this process.

parasitophorous vacuole, then forms a cup (Fig. 1 *C* and *D*); the edges of the cup then approach one another until they fuse (Fig. 1 *E* and *F*). We will refer to this single event as the Big Gulp, defined

as a large [>0.5 fl (μm³) in volume] HV taken up by ring-stage parasites. This structure represented up to 40% of the parasite's cytoplasmic volume (Fig. 2) and was the most common hemoglobin-containing structure found in ring-stage parasites. Images showing the complete serial sectioning of ring-stage parasites taking up the Big Gulp are provided in SI Movies 3–6. In parasites <30 h of age, the Big Gulp accounts for ≈95% of HV volume (data not shown).

Role of Actin During the Big Gulp and FV Formation. The canonical uptake pathways that are morphologically consistent with the Big Gulp include macropinocytosis and phagocytosis (12). Because both require actin polymerization (13), we tested the effects of Cytochalasin D (CytD—a chemical that depolymerizes actin). Infected red blood cells were treated with CytD for 24 h, starting 6 h after invasion (before the Big Gulp occurs; SI Fig. 7). CytD inhibited neither the Big Gulp (data not shown) nor the creation and volume of the FV at the 30-h time point (SI Fig. 8*A Upper*), although it did depolymerize *Plasmodium* actin (SI Fig. 8*B*).

In Trophozoites and Schizonts, the Most Commonly Occurring HVs Are Small. Once the parasite progresses into the trophozoite stage (between 24 and 30 h after invasion—trophozoite-stage parasites are defined as having a FV and one nucleus), a second hemoglobin-uptake process increases its contribution to total hemoglobin uptake (14). This involves the previously characterized electron-dense doughnut-shaped structure, termed the cytostome, which lies flat against the parasite plasma membrane (15–19). Both the parasite plasma membrane and the parasitophorous vacuole membrane invaginate through the cytostome to form a double membrane-bound invagination (Fig. 3*B*). These structures, often more than one per parasite, bud off and form small double membrane-bound small hemoglobin-containing vacuoles (SHV) with an average volume per vesicle only 0.15% that of the average Big Gulp volume. The SHV diameters distribute ≈68 nm (≈ 0.0015
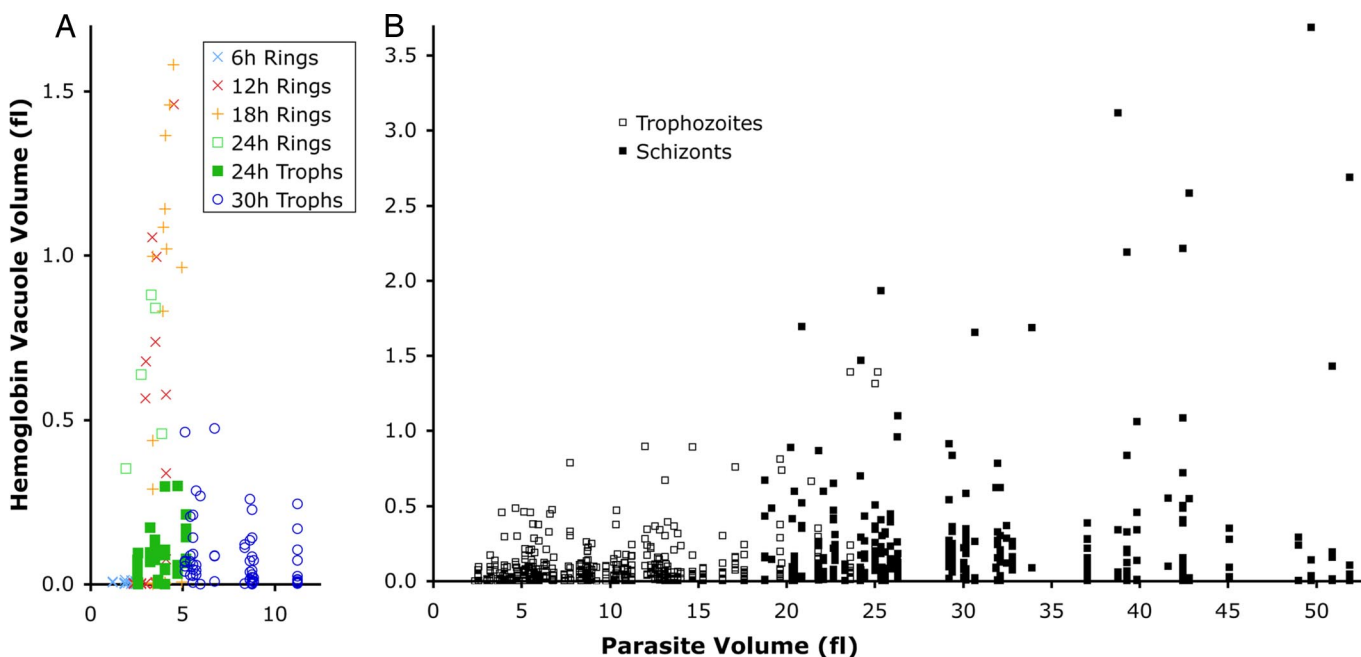

Fig. 2. The distribution of hemoglobin-containing vacuoles compared with parasite volume. Shown are the volumes of completely serial sectioned parasites plotted vs. the volumes of HVs. Parasite stage was determined morphologically. Ring-stage parasites have no FV, trophozoite-stage parasites have one FV and one nucleus, and schizont-stage parasites have multiple nuclei. These stages are loosely correlated with parasite volumes. (*A*) Ring-stage parasites and trophozoites of known age. (*B*) Black squares (open for trophozoites and filled for schizonts) depict the >1,200 HVs from 159 asynchronous control parasites. Large-volume HVs (0.5 fl-1.6 fl) seen in rings correspond to the Big Gulp. Early trophozoites (24 and 30 h in *A*) were not found to contain large-volume HVs (>0.5 fl). As parasites developed they appeared to take up larger HVs, and schizonts frequently contained very large HVs, (0.5–3.7 fl). Such large, actin-independent vesicles are defined as phagotrophs.
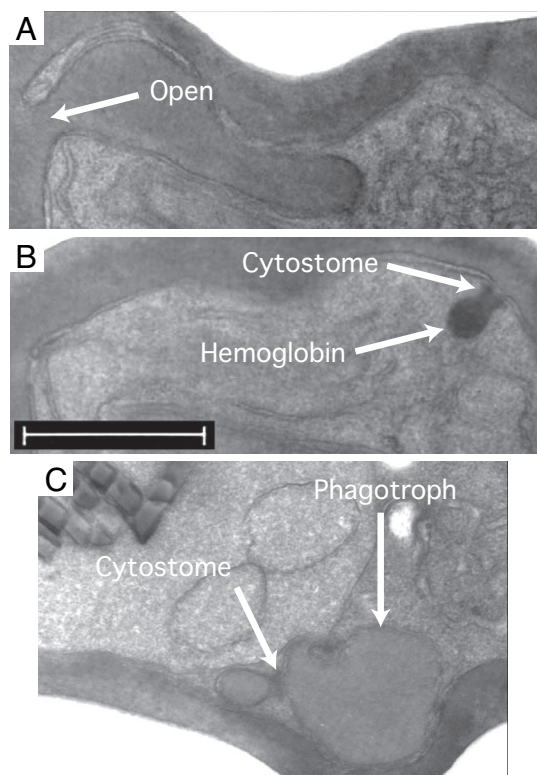
Fig. 3. Morphology of the cytostome and the phagotroph. This figure contains three 100-nm-thick TEM sections showing a portion of two trophozoites living within a red blood cell. A large hemoglobin-containing invagination is shown in *A*, and the opening of the invagination can be seen. This is morphologically distinct from the electron-dense, constricted openings of cytostomes shown in *B* and *C*. Large invaginations are distinguished from phagotrophic vesicles by the fact that phagotrophs are closed off from the red blood cell cytosol. (Scale bar, 1 μm.)

fl) and represent the most commonly occurring HVs in trophozoites and schizonts (SI Fig. 9). These SHVs are consistent in size with non-clathrin-coated vesicles of higher eukaryotes (a diameter of <100 nm or volume <0.004 fl) (20).

Rab5 Regulates Hemoglobin Uptake/Transport. *P. falciparum* expresses three members of the Rab5 family (21), the prototypic marker associated with early endosome formation and transport in other eukaryotes (22). If core eukaryotic endocytic machinery were involved in HV formation and/or transport, then Rab5 would be expected to participate. Parasites stably expressing a constitutively active Rab5a (Q102L) mutant with an N-terminal GFP tag were generated, and the Rab5a was localized by immuno-TEM to SHVs (SI Fig. 10).

Expression of the constitutively active mutant form of Rab5a decreased aggregate HV volume while increasing both the FV volume and the aggregate volume of hemoglobin-uptake structures that remained open to the red blood cell cytosol (SI Table 1). This suggests that Rab5a regulates the process of hemoglobin uptake and transport.

Actin Inhibitors Do Not Interrupt Uptake of Hemoglobin nor Do They Affect HV Volumes. Hemoglobin uptake, transport, and vesicular fusion were explored in trophozoites and schizonts. Synchronized parasites at a time point 36 h after invasion were treated for 4 h with two actin inhibitors, CytD and Jasplankinolide (Jas). These drugs affected *P. falciparum* actin as expected (SI Fig. 8*B*). Although volumes of individual HVs in treated parasites were the same size as in untreated parasites (SI Fig. 11), the combined volume of all

HVs was 3.4-fold greater ($P < 0.001$) under conditions of drug treatment with CytD or 4.3-fold greater ($P < 0.001$) when treated with Jas (SI Fig. 8*A Lower*). In contrast, the FV was 2.2- or 1.8-fold less in volume ($P < 0.001$) when treated with CytD or Jas respectively. Hence, actin polymerization is not necessary for hemoglobin uptake as uptake continues in the presence of actin inhibitors.

The effect of long-term Jas treatment on parasites was investigated. Unsynchronized parasites were treated with Jas for 35 h. This resulted in many vacuoles containing hemozoin (SI Fig. 12), consistent with observations that hemoglobin degrading enzymes are present in HV (ref. 23 and SI Fig. 13).

Cytostomal Tubes. Previous research has implicated cytostomal tubes as major contributors to hemoglobin uptake (15). Cytostomal tubes are long, double membrane-bound tubular invaginations through the cytostome into the parasite cytoplasm (SI Fig. 14 *M–R* and SI Movie 7) that have been suggested to give rise to vesicles from the tube ends (15). Contrary to previous reports, we found that cytostomal tubes did not make a major contribution to hemoglobin uptake. Furthermore, cytostomal tubes appear to bud off and form long double membrane-bound tubular vesicles that were low in volume (< 0.5 fl) and highly elongated (SI Fig. 15 and SI Movie 7). Cytostomal tube formation was only observed in parasites at ≈30 h after invasion (SI Fig. 16). Synchronized parasites treated at 6 h after invasion with CytD and observed at 30 h displayed no cytostomal tubes. This suggests that the actin-dependent transport machinery is required for cytostomal tube formation (SI Fig. 16 and SI Table 2), potentially by mediating elongation of HVs forming from the cytostome.

Late-Stage Parasites Contain Phagotrophs: Unique Large-Volume, Actin-Independent, Hemoglobin-Uptake Vesicles. The most commonly occurring HVs seen in trophozoites and schizonts were SHVs (SI Fig. 9). All other HVs were larger in volume and seen only in larger trophozoites (volume >12 fl) and schizonts (Fig. 2). Smaller trophozoites (volume <10 fl) took up lower-volume HVs than did later stage parasites (volume >12 fl) that contained HVs of up to 3.5 fl in volume (Fig. 2). Such large structures are morphologically consistent with phagosomes (SI Figs. 14 and 17). but, unlike canonical phagosomes (13, 24, 25), their formation was actin-independent (SI Figs. 8 and 11). These structures (Fig. 3*A* and *C*) were typically semispherical or ovoid in shape and morphologically distinct from cytostome-derived SHVs (SI Fig. 17) and cytostomal tubes (SI Fig. 15). Unlike the Big Gulp, there can be multiple large-volume vacuoles in late-stage parasites. We have termed this process phagotrophy (the "eating of nutrients"), a term originally suggested by Rudzinska and Trager (26). Furthermore, we have referred to the resultant large-volume HVs as phagotrophs.

Discussion

Big Gulp Is the Precursor of the FV. In this report of the Big Gulp, we define this structure as a single large (volume >0.5 fl) hemoglobin-containing vacuole taken up by ring-stage parasites not before 6 h after invasion, which happens once, for every ring-stage parasite. We present multiple lines of evidence to suggest that the FV is derived from the Big Gulp rather than from multiple low-volume internalization events, followed by rapid homotypic fusion, as suggested (14, 15): (*i*) In parasites <30 h of age the sum of all small hemoglobin-containing vacuole (SHV) volumes made up only 8% of the average Big Gulp HV volume (data not shown). Intermediate volume HVs (sized between SHVs and Big Gulp HVs) were not seen. Combined, these observations effectively preclude the notion that rapid homotypic fusion of low-volume HVs could form a large HV the size of the Big Gulp, (*ii*) a Big Gulp HV and a FV were never seen in the same parasite, even though a high percentage (67%, 77%, 85%, and 100% of 12-, 18-, 24-, and 30-h parasites, respectively) have either a Big Gulp HV or a FV (SI Fig. 7), and (*iii*)
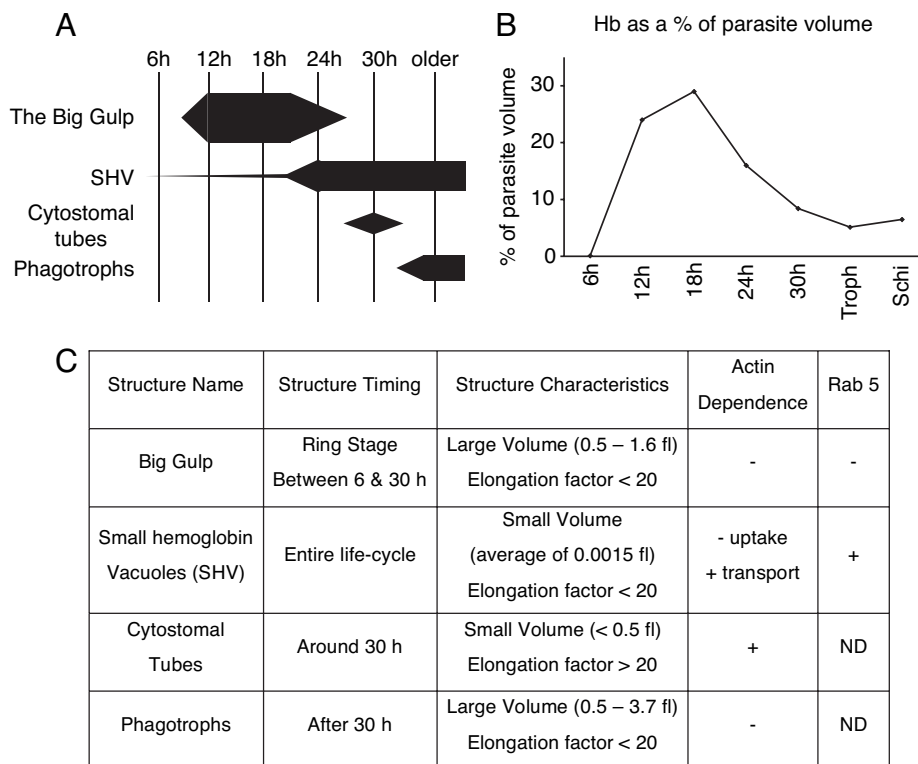
CELL BIOLOGY

Fig. 4. Summary of the four hemoglobin-uptake processes. (*A*) The timing and relative contribution of each hemoglobin-uptake pathway. The thickness of each bar represents the relative total aggregate volume of each of the indicated structures. Each vertical bar sums to 100%. (*B*) Total volume of internal hemoglobin as a percentage of parasite volume, demonstrating the dramatic nature of the Big Gulp. (*C*) Characteristics of the four hemoglobin-uptake structures. All times are given as time after invasion. Elongation factor is defined as the skeletal length of each vacuole divided by its diameter. SHV formation did not depend on actin (−uptake), whereas SHV transport was actin-dependent (+transport). Data not determined was marked ND.

CytD neither inhibited the creation of the FV (data not shown) nor altered the volume of the FV at 30 h (SI Fig. 8*A Upper*), despite blocking transport of HVs (see below). At no time point did 100% of parasites have a Big Gulp. Our presumption is that all parasites create a Big Gulp HV; however, because some parasites had progressed to the trophozoite stage before all parasites had taken the Big Gulp, we are unable to verify this.

Actin Inhibitors Block Transport of HVs to the FV. A 4-h treatment of 36-h parasites with actin inhibitors increased internalized hemoglobin volume and concomitantly decreased FV volume. This suggests either an inhibition of transport of HVs to the FV or an inhibition of HV fusion with the FV. If the latter were true, then the FV would be surrounded by HVs. Our data showed HVs randomly distributed throughout the drug-treated parasites' cytosol, implying that a block in actin function inhibits the transport of HVs but not their formation. We propose that HVs are directed to the FV by transport complexes that contain molecular motors (such as myosins) and membrane-attachment complexes. This would predict that long-term treatment with actin inhibitors (i.e., long-term inhibition of HV transport to the FV) would result in the accumulation of many HVs and/or many hemozoin-containing vesicles, as was observed. Because many smaller, hemozoin-containing vesicles are seen (SI Fig. 12), this also suggests that HVs either contain, or can acquire, all of the molecular machinery required to digest hemoglobin and form hemozoin. In either case, it is clear that hemoglobin is being degraded before FV fusion. Previous work with Plasmepsin II (23) along with data we include here localizing the protease Plasmepsin IV to hemoglobin-uptake structures (SI Fig. 13) further supports this notion.

Rab 5a Is Involved in Hemoglobin Uptake and HV Transport to the FV. Compared with the detailed understanding of endocytic uptake in mammalian cells and yeast, there is a profound lack of understand-

ing of this process in malaria parasites (27). In this regard, the *P. falciparum* genome encodes only a restricted subset of the endocytic machinery present in yeast and mammalian cells (28). Because SHVs, derived from cytostomes, are morphologically consistent with non-clathrin-coated vesicles of higher eukaryotes and bear the core endocytic marker Rab5, they may represent the only conventional endocytic structure in the parasite. Expression of a constitutively active mutant form of Rab5a decreased aggregate HV volume and significantly increased both the FV volume and the aggregate volume of hemoglobin-uptake structures that remained open to the red blood cell cytosol (SI Table 1). This indicated a functional role for Rab5a in hemoglobin transport, likely through increased recruitment of Rab5a effector proteins and/or transport machinery to the parasite surface.

Rab5 regulates homotypic fusion of early endosomes in higher eukaryotes. If it played a similar role in the parasite, a constitutively active mutant of Rab5a might be expected to promote homotypic fusion of SHVs, resulting in an increase in HV volume. In higher eukaryotes, this homotypic fusion is mediated by EEA-1 (29, 30). However, *P. falciparum* contains no EEA-1 homolog (31), and the HV volumes were not altered in the mutant (data not shown). This suggests that SHVs are transported directly to the FV, without intervening fusion.

Big Gulp and Phagotrophy Are Similar. In contrast to the actin-dependence of cytostomal tube formation and of HV transport, the Big Gulp and phagotrophy did not require actin function. These large volume hemoglobin-uptake mechanisms may be mechanistically the same but are temporally distinct; the Big Gulp occurring only once in the ring stage and phagotropy potentially occurring multiple times in the late-trophozoite and schizont stages. Another similarity between these two uptake mechanisms is that both create

a double membrane-bound vacuole. In the case of the Big Gulp, the inner membrane must be removed before this vacuole becomes the FV. Our current methodology does not allow us to define the timing of this event.

The presence of four distinct processes, all of which are associated with hemoglobin uptake, is not parsimonious, despite the fact that they can be unambiguously distinguished from one another by morphology and timing. It is likely that these processes stem from specialized adaptations of the parasite to assimilate to the unique intracellular environment of a red blood cell. The Big Gulp and phagotrophy both deliver hemoglobin in bulk from the erythrocyte cytosol to the parasite. A specialized need for the Big Gulp is likely the formation of the FV, which must be created *de novo*, once and only once, by each intraerythrocytic parasite and which persists as the main lysosomal compartment throughout the intracellular developmental span of the parasite. The vesicular requirements for delivering proteolytic enzymes synthesized and transported through the parasite's secretory pathway to the FV are much different (23). Indeed, in ring-stage parasites and late-stage parasites, in which the Big Gulp and phagotrophy respectively provide the greatest contributions to hemoglobin uptake, the coexistence of SHVs, cytostomal tubes, and larger uptake structures is likely explained by the need to continue transport of proteolytic enzymes to the FV (SI Fig. 13).

The timing, relative contributions to hemoglobin uptake, and morphological characteristics of the four distinct processes described herein are summarized in Fig. 4 and are graphically demonstrated by animation in SI Movie 8. The Big Gulp contributed >92% of ring-stage hemoglobin. In contrast, SHVs derived from cytostomes contributed <8% to total hemoglobin uptake in ring stage parasites, but this contribution rose to >50% of total hemoglobin uptake in trophozoites and schizonts. This comprehensive view of four distinct pathways contributing to hemoglobin uptake and metabolism should open avenues to the study of malaria parasite physiology and drug discovery.

Materials and Methods

Reagents and Parasites. Unless otherwise indicated, all chemicals and enzymes used were obtained from Sigma and New England Biolabs, respectively. The FCR3 strain of *P. falciparum* used was a gift from Dr. Kasturi Haldar (Northwestern University, Chicago).

***In Vitro* Culture of *P. falciparum*.** Parasites were maintained as described (32). Medium was changed daily.

Drug Treatments. Mature schizonts were purified by percoll gradient, diluted to 4% parasitemia 1% hematocrit, and grown for 36 h. At 36 h, 20 μM CytD or 7.5 μM Jas was added, and parasites were grown 4 h before processing for TEM. For timed growth experiments, the above protocol was followed except that drug was added 6 h after schizont purification and samples were taken at designated times.

Cloning of Rab5a cDNA and Construction of *Plasmodium* Expression Plasmids. Plasmodium Rab5a was cloned, and the inverse PCR method (33) was used to generate a dominant-negative mutation resulting in a constitutively activated Rab5a by converting a glutamine at amino acid position 102 in the GTPase domain to a leucine (Q102L).

For GFP expression studies, the mutant (Q102L) Rab5a was subcloned into pGFP-M2-C2. GFP-gene fusions were PCR amplified and cloned into pDONR-21

(Invitrogen) by using the BP reaction and Gateway recombination cloning system (Invitrogen). Subsequent LR reactions (Invitrogen) with the *Plasmodium* Gateway destination vector pHH1-DR0.28-DEST (34) resulted in generation of the *Plasmodium* GFP expression vector pEXP-GFP-Rab5A (Q102L) mutant.

Transfections and Selection of Stable Lines. Transient transfections of malaria parasites with expression constructs were performed by a modification of the previously described preloading technique (35). Packed red blood cells (200 μl) were washed once in ice-cold incomplete cytomix (36) and resuspended to 400 μl in cytomix. Red blood cells were then preloaded with 50 μg of DNA by electroporation. To obtain a stable GFP-Rab5A(Q102L) mutant line, transfected parasites were selected in 2.2 μM methotrexate for 4 weeks.

Immunoelectron Microscopy. Parasite cultures were pelleted and resuspended in fixative containing 4% paraformaldehyde, 0.1% glutaraldehyde, and 0.25 M Hepes (pH7.4) for 1 h at 25°C. Samples were washed and resuspended in 500 μl of melted 10% bovine gelatin. Samples were pelleted and iced for 1 h, cut out of the tubes, and placed in 7.5 M sucrose and 10% polyvinyl-pirolidone. After 24 h at 4°C, samples were placed onto pins and frozen in liquid nitrogen. Sections were cut in a −90°C ultramicrotome and placed onto grids, preblocked in PBS containing 5% BSA, and stained with a 1:100 dilution of rabbit anti-GFP (Molecular Probes) washed three times and stained with 5-nm gold goat anti-rabbit IgG (Electron Microscopy Sciences).

Electron Microscopy. Samples were fixed, washed, and resuspended in 500 μl of 0.2 M cacodylate containing 8% BSA and pelleted. Four drops of 25% glutaraldehyde were added, without mixing, and samples were set to gel for 1 h before pellets were cut out of the tubes. Samples were processed as described (9).

Volume Calculations. Digital images were acquired of all of the serial sections that contained a specific parasite. Images were aligned with AutoAligner 2.0.0 (Bitplane AG). Photoshop 9 (Adobe) was used to identify and color structures as appropriate (SI Fig. 5). Determinations of hemoglobin-containing structures still open to the red blood cell cytosol could be made only by looking at every TEM section that contained part of that structure. SI Fig. 5*B* shows hemoglobin-containing structures that were open to the outside, and Fig. 5C shows HVs. Hemoglobin identification was confirmed by serial immuno-TEM (SI Fig. 6). Images were segmented, the datasets were loaded into Volocity 3.1 (ImproVision) to measure organellar volumes, geometries, and to create three-dimensional models (SI Movie 2). Pixels had a known volume, with the *X* and *Y* dimensions being determined from the resolution and magnification of the digital camera and the *Z* dimension being the thickness of the TEM section. Volocity then counted all pixels within a structure and multiplied by the known volume of each pixel. Volumes measured by Volocity in μm^3 (a unit of area) have been expressed in femtoliters (fl, a unit of volume). Other than volume, the geometric data measured are skeletal length (SL), defined as the maximum length in the object as determined by eroding evenly from an object's borders inward until only a one-voxel skeleton remains, and skeletal diameter (SD), defined as the average diameter of an object along the measured SL. All other calculations were preformed in Excel 11.1.1 (Microsoft).

1. Goodyer ID, Pouvelle B, Schneider TG, Trelka DP, Taraschi TF (1997) Characterization of macromolecular transport pathways in malaria-infected erythrocytes. *Mol Biochem Parasitol* 87:13–28.
2. Francis SE, Sullivan DJ, Jr, Goldberg DE (1997) Hemoglobin metabolism in the malaria parasite *Plasmodium falciparum*. *Annu Rev Microbiol* 51:97–123.
3. Egan TJ, *et al.* (2002) Fate of haem iron in the malaria parasite *Plasmodium falciparum*. *Biochem J* 365:343–347.
4. Liu J, Istvan ES, Gluzman IY, Gross J, Goldberg DE (2006) *Plasmodium falciparum* ensures its amino acid supply with multiple acquisition pathways and redundant proteolytic enzyme systems. *Proc Natl Acad Sci USA* 103:8840–8845.
5. Saliba KJ, Kirk K (2001) Nutrient acquisition by intracellular apicomplexan parasites: Staying in for dinner. *Int J Parasitol* 31:1321–1330.
6. Slomianny C, Prensier G, Charet P (1985) Ingestion of erythrocytic stroma by *Plasmodium chabaudi* trophozoites: Ultrastructural study by serial sectioning and 3-dimensional reconstruction. *Parasitology* 90 (Pt 3):579–88.
7. Aikawa M (1971) Parasitological review. *Plasmodium*: The fine structure of malarial parasites. *Exp Parasitol* 30:284–320.
8. Aikawa M, Hepler PK, Huff CG, Sprinz H (1966) The feeding mechanism of avian malarial parasites. *J Cell Biol* 28:355–373.
9. Elliott DA (2007) Serial sectioning via microtomy (or, how to get over 100 consecutive serial sections on one TEM grid). *Microscopy Today* 15:30–33.

CELL BIOLOGY

10. Krogstad DJ, Schlesinger PH, Gluzman IY (1985) Antimalarials increase vesicle pH in *Plasmodium falciparum*. *J Cell Biol* 101:2302–2309.

11. Yayon A, Cabantchik ZI, Ginsburg H (1984) Identification of the acidic compartment of *Plasmodium falciparum*-infected human erythrocytes as the target of the antimalarial drug chloroquine. *EMBO J* 3:2695–2700.

12. Mukherjee S, Ghosh RN, Maxfield FR (1997) *Endocytosis Physiol Rev* 77:759–803.

13. May RC, Machesky LM (2001) Phagocytosis and the actin cytoskeleton. *J Cell Sci* 114:1061–1077.

14. Langreth SG, Jensen JB, Reese RT, Trager W (1978) Fine structure of human malaria *in vitro*. *J Protozool* 25:443–452.

15. Slomianny C (1990) Three-dimensional reconstruction of the feeding process of the malaria parasite. *Blood Cells* 16:369–378.

16. Slomianny C, Prensier G (1990) A cytochemical ultrastructural study of the lysosomal system of different species of malaria parasites. *J Protozool* 37:465–470.

17. Slomianny C, Charet P, Prensier G (1983) Ultrastructural localization of enzymes involved in the feeding process in *Plasmodium chabaudi* and *Babesia hylomysci*. *J Protozool* 30:376–382.

18. Yayon A, Timberg R, Friedman S, Ginsburg H (1984) Effects of chloroquine on the feeding mechanism of the intraerythrocytic human malarial parasite *Plasmodium falciparum*. *J Protozool* 31:367–372.

19. Cox FE, Vickerman K (1966) Pinocytosis in *Plasmodium vinckei*. *Ann Trop Med Parasitol* 60:293–296.

20. Nichols BJ, Lippincott-Schwartz J (2001) Endocytosis without clathrin coats. *Trends Cell Biol* 11:406–412.

21. Quevillon E, *et al.* (2003) The *Plasmodium falciparum* family of Rab GTPases. *Gene* 306:13–25.

22. Seabra MC, Coudrier E (2004) Rab GTPases and myosin motors in organelle motility. *Traffic* 5:393–399.

23. Klemba M, Beatty W, Gluzman I, Goldberg DE (2004) Trafficking of plasmepsin II to the food vacuole of the malaria parasite *Plasmodium falciparum*. *J Cell Biol* 164:47–56.

24. May RC, Caron E, Hall A, Machesky LM (2000) Involvement of the Arp2/3 complex in phagocytosis mediated by FcgammaR or CR3. *Nat Cell Biol* 2:246–248.

25. Defacque H, *et al.* (2002) Phosphoinositides regulate membrane-dependent actin assembly by latex bead phagosomes. *Mol Biol Cell* 13:1190–1202.

26. Rudzinska MA, Trager W (1959) Human malaria parasites in continuous culture. *J Biophys Biochem Cytol* 6:103–112.

27. de Castro FA, *et al.* (1996) Identification of a family of Rab G-proteins in *Plasmodium falciparum* and a detailed characterisation of pfrab6. *Mol Biochem Parasitol* 80:77–88.

28. Joiner KA, Roos DS (2002) Secretory traffic in the eukaryotic parasite *Toxoplasma gondii*: Less is more. *J Cell Biol* 157:557–563.

29. Gorvel JP, Chavrier P, Zerial M, Gruenberg J (1991) rab5 controls early endosome fusion *in vitro*. *Cell* 64:915–925.

30. Barbieri MA, *et al.* (1998) Evidence for a symmetrical requirement for Rab5-GTP in *in vitro* endosome-endosome fusion. *J Biol Chem* 273:25850–25855.

31. McIntosh MT, *et al.* (2007) Traffic to the malaria parasite food vacuole: A novel pathway involving a phosphatidylinositol 3-phosphate-binding protein. *J Biol Chem* 282:11499–11508.

32. Trager W, Jensen JB (1976) Human malaria parasites in continuous culture. *Science* 193:673–675.

33. Hemsley A, Arnheim N, Toney MD, Cortopassi G, Galas DJ (1989) A simple method for site-directed mutagenesis using the polymerase chain reaction. *Nucleic Acids Res* 17:6545–6551.

34. Skinner-Adams TS, Hawthorne PL, Trenholme KR, Gardiner DL (2003) GATEWAY vectors for *Plasmodium falciparum* transfection. *Trends Parasitol* 19:17–18.

35. Deitsch K, Driskill C, Wellems T (2001) Transformation of malaria parasites by the spontaneous uptake and expression of DNA from human erythrocytes. *Nucleic Acids Res* 29:850–853.

36. van den Hoff MJ, Moorman AF, Lamers WH (1992) Electroporation in ''intracellular'' buffer increases cell survival. *Nucleic Acids Res* 20:2902.